

## Polarization of impurity emission lines from a tokamak plasma

Takashi Fujimoto,<sup>1</sup> Hironori Sahara,<sup>1</sup> Tetsuya Kawachi,<sup>1,\*</sup> Thomas Kallstenius,<sup>1,†</sup> Motoshi Goto,<sup>1</sup> Hiroshi Kawase,<sup>1</sup>  
Takeo Furukubo,<sup>1</sup> Takashi Maekawa,<sup>2</sup> and Yasushi Terumichi<sup>2</sup>

<sup>1</sup>*Department of Engineering Science, Faculty of Engineering, Kyoto University, Kyoto 606-01, Japan*

<sup>2</sup>*Department of Physics, Faculty of Science, Kyoto University, Kyoto 606-01, Japan*

(Received 30 May 1996)

The visible-uv spectrometer was equipped with a double refracting calcite plate for the purpose of resolving a spectral line into the two linearly polarized components and observing these components simultaneously. Relative intensities of these components have been measured for heliumlike carbon and berylliumlike oxygen impurity lines from the WT-3 tokamak plasma at Kyoto University. In the joule heating mode, for transition from the joule heating to the lower-hybrid current drive mode, and for application of the electron cyclotron heating, changes in the relative intensities were found, which indicated that these lines were polarized. Implications of the polarization of the emission lines from plasma are discussed. [S1063-651X(96)51809-X]

PACS number(s): 52.25.Tx, 52.70.Kz, 32.70.-n

In spectroscopy of magnetically confined plasmas emission radiation is assumed to be unpolarized, except in the cases of the observation of Zeeman or Stark split lines [1,2]. However, if an “ordinary” emission line were polarized, this has significant implications in spectroscopy; that is, besides the intensity and the spectral profile of the line we are able to use its polarization characteristics in interpreting the plasma. Since the polarization results from the spatial anisotropy of the plasma, its characteristics, i.e., the degree and direction of polarization, would give us quantitative information concerning the anisotropic, and therefore, nonthermal, properties of the plasma [3,4].

The WT-3 tokamak at Kyoto University had the major and minor radii of 0.65 and 0.21 m, respectively, and the toroidal magnetic field was 1.5 T at the poloidal center. A plasma was produced in the joule heating (JH) mode with the toroidal current of 60 kA to reach a stationary state at the one turn loop voltage of 4 V. At 30 ms after the start the lower-hybrid wave of 2 GHz with 150 kW was injected and the current was sustained in the lower-hybrid current drive (LHCD) mode with virtually no loop voltage. At 50 ms the electron cyclotron wave of 56 GHz with 150 kW was superimposed [electron cyclotron heating (ECH)]. The location of the launcher of the LH wave was at 135° counterclockwise (seen from the above) with respect to the observation port for the visible-uv spectroscopy, and that of the EC wave was at 22.5°. The electron density was measured by the far infrared interferometer to be typically  $3 \times 10^{18} \text{ m}^{-3}$  at the plasma core, and the electron temperature was estimated from the electron cyclotron emission intensities to be 100–300 eV.

The deviation of the magnetic field direction from the toroidal direction was 7° in the outermost plasma region. Since we observed emission lines from multiply ionized ions present in the plasma core regions, the deviations there were expected to be much smaller. By ignoring these deviations

we took the quantization axis in the toroidal direction. We assumed the axial symmetry around the quantization axis, since any asymmetry created in the ensemble of ions was smoothed out owing to their fast Larmor precession. Then the polarized components of the emission lines were the  $\pi$  light (having the electric fields oscillating in the direction of the quantization axis) and the  $\sigma$  light.

The plasma was observed slightly from above the equatorial plane. The optical axis defined by the spectrometer crossed the center of the plasma core, which was displaced by 4 cm to the major radius direction. The plasma radiation went through a window of a 15-mm-thick fused quartz plate and five steering mirrors, to be focused on the entrance slit of the spectrometer. On the opposite side wall of the plasma vessel a light damp made of knife edge blades was installed. Distortions of the polarization characteristics of the transmitted light through the window were examined. The first cause of distortion was the photoelastic effect: The mechanical stress due to the atmospheric pressure caused birefringence to the fused quartz. The magnitude of distortions was calculated and found to be largest in the regions near the four corners of the rectangular window. The  $p$  wave ( $\sigma$  light), taken for the purpose of illustration, incident on the plate with the incidence angle 20° (with respect to the surface normal), became an elliptically polarized light during the transmission, giving rise to the  $s$ -wave component. The maximum intensity of the secondary  $s$ -wave component was less than 2% of the primary  $p$ -wave intensity near the corners for the shortest wavelength (220 nm) of the lines observed. We confirmed the above estimate by using a diode laser: Linearly polarized light was incident on the window from outside, and after passing through the plate twice and being reflected back by its inner surface, the polarization characteristics of the light were examined. It indicated no more distortion than 0.2%, as calculated for the wavelength of 635 nm with the incidence angle of 30° for this particular experiment. In our observations described later we used only the region of the window near its center, where the distortion was absent. The magnetic field at the window was estimated to be about 0.1 T in the direction at 20° with respect to the toroidal direction. The component of this field in the direc-

\*Present address: The Institute of Physical and Chemical Research (RIKEN), Hirosawa, Wako, Saitama 351-01, Japan.

†Present address: Ericsson Components AB, S-16481 Kista, Sweden.

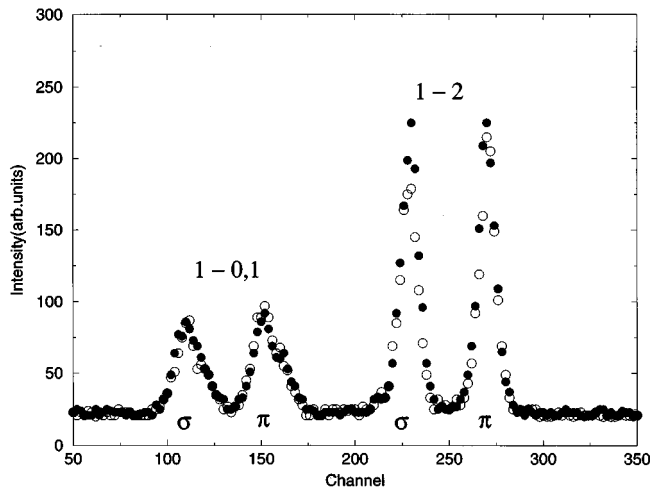


FIG. 1. Polarization resolved spectra of heliumlike carbon lines,  $C\text{v}(2s^3\ S_1-2p^3\ P_{0,1,2})$  observed from plasmas in the joule heating mode for different shots. The two peaks at right are the  $\pi$  (rhs peak) and  $\sigma$  (lhs peak) polarized components of the  $J=1-J=2$  line. The weaker lines ( $J=1-J=0,1$ ) are unresolved and the  $\pi$  and  $\sigma$  components each appear as aggregates.

tion of the light path was  $10^{-3}$  T or less, and the Faraday effect tilted the plane of linear polarization direction by less than  $0.1^\circ$  during the transmission through the plate (for 220 nm). The Voigt effect or the Cotton-Mouton effect gave rise to a distortion of  $10^{-8}$ . All of these distortions were small and ignored.

The incidence angles of the light to the steering mirrors were  $3^\circ$ – $45^\circ$ . The linear polarization of the plasma radiation was in all the cases in the direction parallel ( $p$  wave) or perpendicular ( $s$  wave) to the plane of incidence of the mirrors. The reflection efficiencies of these mirrors for these polarized components would be different, but no mixing of the original polarizations occurred.

The spectrometer had 1 m focal length and  $f/10$ . The grating was of 3600 grooves/mm, giving the reciprocal linear dispersion of 0.22–0.25 nm/mm at 220–280 nm. The entrance slit width was 0.1 mm, and the dispersed light was detected by a multichannel detector (Tracor–Northern TN-6130,  $12.8 \times 2.5$  mm). It had 512 channels and we used channels with even channel numbers. The wavelength width per channel was 0.005 nm/channel at 220 nm. Just behind the entrance slit we placed a calcite plate with thickness of 5.4 mm. The crystal optic axis was in the horizontal direction at  $60^\circ$  with respect to the normal, and the normal incident light was separated into the ordinary ( $o$ ) ray and the extraordinary ( $e$ ) ray. After transmission the  $e$  ray (the  $\pi$  light) was displaced parallel from the  $o$  ray ( $\sigma$  light) by 1.1 mm horizontally, and the image of the entrance slit was focused by these rays at different locations (1.1 mm apart) on the detector. Examples of the images are seen in Figs. 1–3. Distortion of the images caused by the insertion of the calcite plate was within the tolerable level. The ratio of the apparent intensities of these two components is a measure of polarization of this line. For the purpose of detecting any artificial apparent polarization due to blending of closely lying weak lines, we repeated the measurement with the calcite plate rotated by  $180^\circ$  around its horizontal axis. In this way, the relative po-

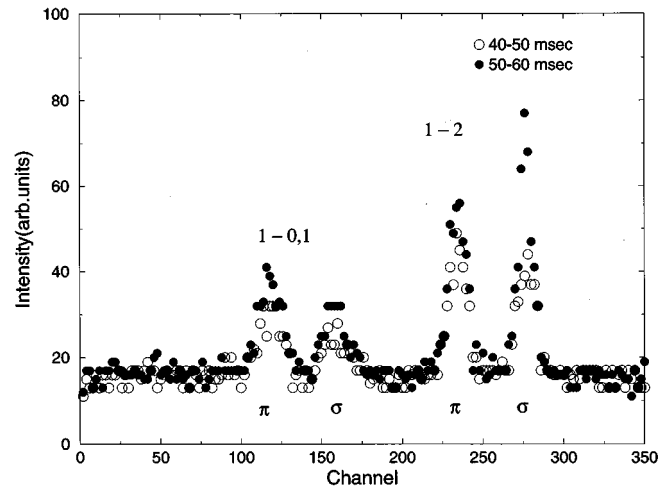


FIG. 2. Polarization resolved spectra of heliumlike carbon,  $C\text{v}(2s^3\ S_1-2p^3\ P_{0,1,2})$  observed from plasmas in the lower-hybrid current drive mode ( $\circ$ ) and in the (lower-hybrid current drive + electron cyclotron heating) mode ( $\bullet$ ). The relative positions of the  $\pi$  and  $\sigma$  components have been interchanged from Fig. 1.

sitions of the  $e$ - and  $o$ -ray images were interchanged, and thus any blending effect would appear in the opposite sense, making it easier to detect the artificial “polarization.”

We could not calibrate the relative sensitivities of our detection system, including the window and the mirrors, for the different polarized components. Emission lines of atoms and ions for transition with the upper level having total angular momentum  $J$  (or  $F$ ) = 0 or  $\frac{1}{2}$  are never polarized, and could be used for the purpose of calibration. However, it turned out that these lines were too weak, as is expected from the  $LS$  coupling line strength, or were blended with other lines, making its isolation difficult. In the following, therefore, we present our result in terms of the apparent relative intensities of the two polarized components.

During one discharge lasting over 100 ms we observed the emission lines over each 10 ms time segment, which consisted of 7.44 ms for the net integration time of the signal and 2.56 ms for signal transfer. We observed several lines from intrinsic impurity oxygen and carbon ions in various ionization stages for 45 shots of discharge. We also observed some of the lines for ten shots of discharge of the JH and JH+ECH modes. Each shot produced ten frames of spectrum. We examined all of them, and found changes of relative intensities of the  $\pi$  and  $\sigma$  components, indicating a change in the polarization degree, during the course of time or for different shots. In some cases, however, the signal intensities were too weak to draw a definite conclusion, or in some other cases, the apparent polarization change might be attributed to the blending effect. We excluded these suspicious cases, then we had about 50 frames of spectrum left, with which we could not deny the existence of polarization. A few examples are shown in the following.

Figure 1 shows two spectra of heliumlike carbon lines:  $C\text{v}(2s^3\ S_1-2p^3\ P_{0,1,2})$  for different shots. Both of them are for the JH mode (20–30 ms after the start of discharge). The weaker lines [227.792 nm ( $J=1-J=1$ ) and 227.725 nm ( $1-0$ )] are not separated, and the  $\pi$  components and the

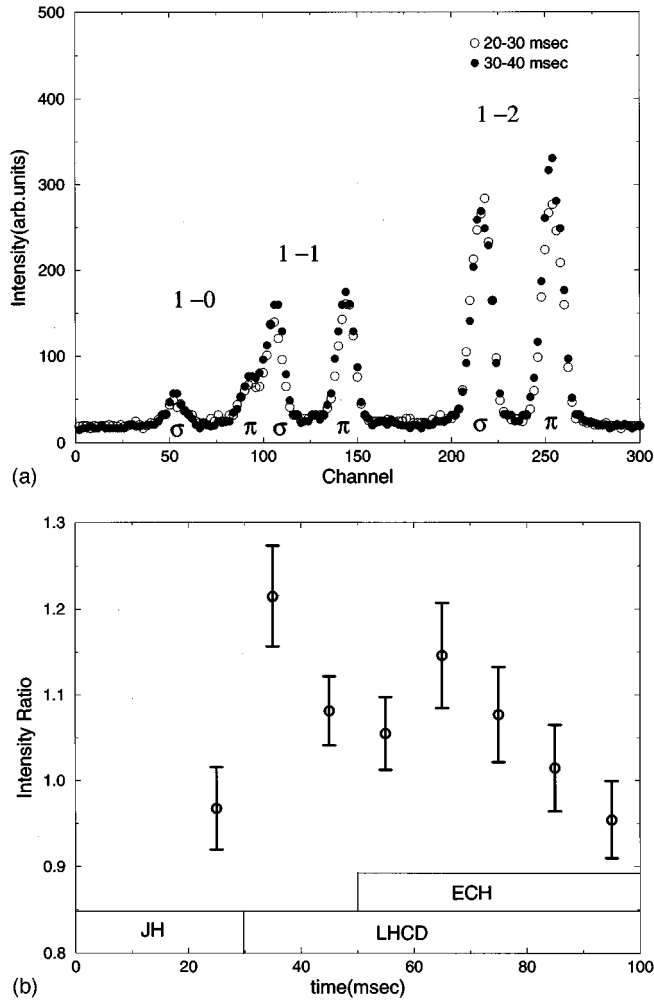


FIG. 3. (a). Polarization resolved spectra of berylliumlike oxygen, O V ( $3s\ ^3S_1-3p\ ^3P_{0,1,2}$ ) observed from plasmas in the joule heating mode ( $\circ$ ) and in the lower-hybrid current drive mode ( $\bullet$ ). The two peaks at right are the  $\pi$  and  $\sigma$  polarized components of the  $J=1-J=2$  line. (b). The apparent intensity ratio of the  $\pi$  component to the  $\sigma$  component of the  $J=1-J=2$  line during the course of time, indicating changes of the polarization degree.

$\sigma$  components each appear as aggregates. The  $\pi$  component of the strongest line, 227.091 nm (1-2), is, for one of the shots, substantially stronger than the  $\sigma$  component; this feature is common for many JH plasmas. The other spectrum shows almost equal apparent intensities for both of the polarized components. This indicates that in one of the shots, or even in both of them, this line is polarized.

The second example is shown in Fig. 2. This shows again the heliumlike carbon lines; the calcite plate has been turned over, so that the  $\pi$  component appears on the left-hand side of the  $\sigma$  component. This figure illustrates the transition from the LHCD mode to the LHCD+ECH mode. Before the application of ECH the  $\pi$  component of the line 1-2 is stronger, but after that the situation is reversed.

Figure 3(a) shows the spectra of berylliumlike oxygen for transition of discharge from the JH mode to the LHCD mode. The lines are triplet O V ( $3s\ ^3S_1-3p\ ^3P_{0,1,2}$ : 278.985, 278.699, and 278.101 nm). The relative line strengths of these lines in the *LS* coupling scheme are 1:3:5.

The  $\pi$  component of the first line and the  $\sigma$  component of the second line merge. For the strongest line ( $J=1-J=2$ ), the ratio of the apparent intensities of the  $\pi$  component to the  $\sigma$  component increases in the LHCD mode as compared with that in the JH mode. Figure 3(b) shows the temporal development of the apparent intensity ratio for this shot. The first and second points correspond to the spectra in Fig. 3(a). The intensity ratio could not be determined in the first two 10 ms segments because the intensities were too weak.

We now examine experimental uncertainties. In Figs. 1-3 one unit of intensity in the ordinate for one channel corresponds approximately to  $10^3$  photons. If we take into account the quantum efficiencies of the multichannel plates of our detector, that number would decrease by an order, which would be the number of the photoelectrons contributing to the signal intensity of this channel. Thus, for signals with 100 units the statistical uncertainties are insignificant. For weaker lines like the  $J=1-J=0,1$  lines in Fig. 2 uncertainties would be substantial, due partly to the background.

As mentioned earlier, we were extremely careful about possible line blending; i.e., one of the polarized components of a line of interest may be blended with another component of a nearby line, enhancing the apparent intensity of the former component. An example of this possibility is seen in Fig. 3(a); in the JH mode discharge, several very weak lines appear in the region of the 1-0 and 1-1 lines. For example, if the small peak at about channel 176 were the  $\sigma$  component of an unidentified line, its  $\pi$  component would have contributed to the  $\sigma$  component intensity of the 1-2 line. If this were the case, and if the relative intensities of the polarized components of this weak line are about equal, our point in Fig. 3(b) for 20-30 ms would have been decreased by 2% from the true value. The resulting relative intensity in this particular example, however, lies within the estimated uncertainty. This blending difficulty would be eliminated if we adopt an experimental arrangement in which we observe the two polarized components with two independent detectors.

We have observed the polarization of ‘‘ordinary’’ lines emitted from a magnetically confined plasma. Since the lines were observed with all their Zeeman and Stark components included, we conclude that in one or both of the cases in Figs. 1-3 these lines are polarized. This means that the ensemble of the excited ions in the upper level is polarized under these plasma conditions; more specifically, these ions are aligned. Since the present plasma is in the ionizing plasma phase [5] and since the opacity effect is insignificant [6], the origin of this *alignment* should be spatially anisotropic collisional excitation by electrons having an anisotropic velocity distribution. An example of anisotropic distribution is a Maxwellian distribution with different temperatures in different directions [3,7]. Another example is the existence of a beam component or a ‘‘tail’’ superimposed on bulk electrons having an isotropic distribution [8]. A specific ‘‘shape’’ of the electron velocity distribution gives rise to a specific set of population and alignment in various excited levels of ions, or a set of intensity and polarization of emission lines from these levels. For the shots shown in Fig. 1 we found that the second shot showed slightly noisier and higher x-ray signals compared with other shots. This suggests that the electron velocity distribution in the second plasma is different from the other shots.

In order to relate our observation of population and alignment to the velocity distribution, we have to interpret them in terms of a kinetic model that takes into account the spatial anisotropy of the electron velocity distribution. We call this model the alignment collisional-radiative (CR) model. This model consists of two parts: a CR model for population, which is similar to the conventional CR model [9], and a CR model for alignment. The full account of the basic formulation of the alignment CR model and its application to experiment will be published in a separate paper.

Another point to be noted is concerning the *observed intensity*. We take the plasma shown by Fig. 2 for the purpose of illustration. We assume that, during 40–50 ms, the plasma is isotropic and all the lines are unpolarized. That means our detection system is more sensitive to the  $\pi$  component by about 20%. Then, during the 50–60 ms period, the  $\sigma$  component of the 1–0,1 lines has almost the same intensity as the  $\pi$  component, while the  $\sigma$  component of the 1–2 line is about 1.8 times more intense than the  $\pi$  component. Suppose we perform three experiments of conventional intensity spectroscopy on this plasma. In the first experiment we observe the plasma from the direction perpendicular to the quantization axis, as in the present experiment, with a detection system that is sensitive only to one of the linearly polarized components, say, the  $\pi$  component in the present geometry; this last assumption is not entirely unrealistic when we use a grating or crystal spectrometer. The observed spectrum

would be something like the  $\pi$  peaks in Fig. 2. In the second experiment we rotate our detection system around the optical axis of the spectrometer by  $90^\circ$ , then we would obtain a spectrum similar to the  $\sigma$  peaks in Fig. 2. In this spectrum the intensity of the 1–2 line is 1.8 times stronger than that in the first spectrum. The polarized component has a spatially anisotropic intensity distribution: The  $\pi$  component has the distribution proportional to  $\sin^2\theta$  and the  $\sigma$  component to  $2 - \sin^2\theta$ , where  $\theta$  is the polar angle with respect to the quantization axis. The third experiment is that we observe the plasma from the direction of the quantization axis,  $\theta=0$ , with the same detection system. Under the present assumption of axial symmetry, the result would be exactly the same as that of the second experiment. On the other hand, if our detection system had equal sensitivities for the two polarized components, the above three experiments would give intensity of the 1–2 line to be 1.4 [ $=(1+1.8)/2$ ], 1.4, and 1.8, respectively. Thus, the *observed intensity* ranges from 1 to 1.8 depending on the experimental geometry and the characteristics of the detection system. The *true intensity* that represents the *population* is given by  $[I(\pi) + 2I(\sigma)]/3$ , or 1.5 in this example. The above arguments indicate the importance of the polarization phenomena even in the conventional intensity spectroscopy.

This work was supported partly by Grand-in-Aid for Scientific Research on Priority Areas and that for Co-operative Research.

- 
- [1] D. Wróblewski, L. K. Huang, H. W. Moos, and P. E. Phillips, Phys. Rev. Lett. **61**, 1724 (1988).
- [2] A. Boileau, M. von Hellermann, W. Mandl, H. P. Summers, H. Weisen, and A. Zinoviev, J. Phys. B **22**, L145 (1989).
- [3] J. C. Kieffer, J. P. Matte, H. Pépin, M. Chaker, Y. Beaudoin, T. W. Johnston, C. Y. Chien, S. Coe, G. Mourou, and J. Dubau, Phys. Rev. Lett. **68**, 480 (1992); J. C. Kieffer, J. P. Matte, M. Chaker, Y. Beaudoin, C. Y. Chien, S. Coe, G. Mourou, J. Dubau, and M. K. Inal, Phys. Rev. E **48**, 4648 (1993).
- [4] S. A. Kazantsev and J.-C. Hénoux, *Polarization Spectroscopy of Ionized Gases* (Kluwer, Dordrecht, 1995).
- [5] T. Fujimoto, J. Phys. Soc. Jpn. **47**, 265 (1979).
- [6] T. Kawachi, K. Murai, G. Yuan, S. Ninomiya, R. Kodama, H. Daodo, Y. Kato, and T. Fujimoto, Phys. Rev. Lett. **75**, 3826 (1995).
- [7] M. D. Bowden, T. Okamoto, F. Kimura, H. Muta, K. Uchino, K. Muraoka, T. Sakoda, M. Maeda, Y. Manabe, M. Kitagawa, and T. Kimura, J. Appl. Phys. **73**, 2732 (1993).
- [8] L. Pieroni and S. E. Segre, Phys. Rev. Lett. **34**, 928 (1975); B. Coppi, F. Pegoraro, R. Pozzoli, and G. Rewoldt, Nucl. Fusion **16**, 309 (1976).
- [9] D. R. Bates, A. E. Kingston, and R. W. P. McWhirter, Proc. R. Soc. London **267**, 297 (1962).